Effect of Porogenic Agent Type and Firing Temperatures on Properties of Low-Cost Microfiltration Membranes from Kaolin

Mouafon Mohamed, Dayirou Njoya, Mohamed Hajjaji, André Njoya, Gisèle Laure Lecomte-Nana, Daniel Njopwouo

Effect of Porogenic Agent Type and Firing Temperatures on Properties of Low-Cost Microfiltration Membranes from Kaolin

Mouafon Mohamed,[a] Njoya Dayirou,[a,*] Hajjaji Mohamed,[b] Njoya André,[c] Lecomte-Nana Gisèle Laure[d] and Njopwouo Daniel[a]

[a]Applied Inorganic Chemistry Laboratory, Department of Inorganic Chemistry, Faculty of Sciences, University of Yaoundé 1, P.O. Box: 812 Yaoundé, Cameroon

[b]Laboratory of Materials Physicochemistry and Environment, Department of Chemistry, Faculty of Sciences Semlalia Marrakech, University of Cadi Ayyad, Boulevard Prince Moulay Abdellah, BP: 2390 – 40000 Marrakech, Maroc

[c]Institute of Fine Arts of Foumban, University of Dschang, BP: 31 Foumban, Cameroon

[d]Research Institute on Ceramics, University of Limoges, CEC, 12 Rue Atlantis 87068 Limoges, France.

ABSTRACT

The present work is focused on the development and characterization of low-cost flat microfiltration ceramic membranes from West Cameroonian kaolin, cassava starch and bovine bone ash as pore-forming agents, and comparative study of porogens' influence on membranes properties. These materials were chosen due to their abundance in the country and their beneficial properties. The proportion of porogens varied from 0% (CM0) to 20% and all samples were treated at 1000°-1150°C; membranes without porogenic agent (CM0) gave good results. Linear shrinkage and weight loss values were <7% and <30%, respectively. SEM pictures revealed that inter-granular contacts were formed at 1150°C for all the samples and thus materials densification was more important. Porosity varied between 31% and 52% at 1150°C, and flexural strength increased from 1.07 to 7.79 MPa. Samples containing bovine bone ash contributed to the improvement of membrane microstructure, mechanical and corrosion resistance. Filtration tests through CM04 and CM34 gave turbidity rejection factors of 97.70% and 99.26%, respectively. Decisively, good and low-cost microfiltration ceramic membrane can be developed by using cassava starch and bovine bone ash as porogenic agents.

[Keywords: Kaolin, Bovine bone, Cassava starch, Ceramic membranes, Filtration test]

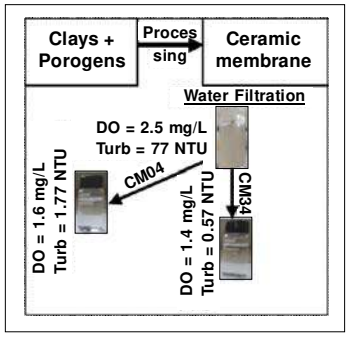

Introduction

Clays are generally used for water and wasewater treatment through adsorption and filtration methods.[1, 2] Valorization of clays in the elaboration of porous ceramics have attracted increasing interest due to their applications as separation media for molten metals, hot gases, varieties of liquid filtration process, as catalyst supports, bone scaffolds and electrodes in fuel cells.[3–7] They are used in many industries for water and wastewater treatment as microfiltration, ultrafiltration or nanofiltration membrane.[8–12] The use of ceramic membranes has many advantages such as high thermal and chemical stability, pressure resistance, long lifetime, good resistance in fouling, and ease of cleaning.[5, 11–17] The mechanical strength of double layer membranes is provided by the support.[11, 14, 18]

*Corresponding author; email: dnjoya@uy1.uninet.cm, dayirou2000@yahoo.fr

Unfortunately, commercial ceramic membranes prepared from alumina, titania, zirconia and silica are too expensive for application in environmental technology which require high permeation flux and low cost to treat large volumes of dust-containing hot gas and industrial wastewater.[9, 11] This drawback is observed through the society and precisely in the household level, where ceramic membranes are not widely used due to their high cost. Recently, significant efforts have been put to develop new types of low-cost inorganic membranes by using cheaper raw materials,[14] natural clay,[9, 16, 19–24] natural pozzolana,[24] animal bone,[25] starch[26, 27] and cordierite.[5, 28] Animal bone and starch are used as porogenic agents. Many authors have produced asymmetric membranes by using only one porogenic agent (synthetic and natural organic and inorganic materials are used). Despite the abundance of natural pore-forming agents and their low price, the choice of one, which can also contribute to improving other properties such as mechanical and chemical resistance

of desired ceramic membrane, remains difficult. Thus the challenge of this work is to study the effects of temperature, and organic (cassava starch) and inorganic (bovine bone ash) porogenic agents on the microstructure, physico-chemical and mechanical properties of the ceramic membrane. In west Cameroon, precisely at Mayouom and Koutaba, there are large clay deposits. Many studies carried out on these clays are focused on the elaboration of porcelain, stoneware and vitreous ceramics.[29–31]

The aim of the present study is to produce low-cost ceramic membranes based on natural Cameroonian clay from Mayouom and Koutaba, bovine bone ash, cassava starch, and to test their performance in the purification of polluted water. Bovine bone ash and starch were added as pore-forming agents to produce enough porosity with acceptable mechanical properties. Starch and bovine bone were chosen as porogenic agents due to their abundance in the country, their relatively low cost and their ability to release CO_2 simultaneously with pore-forming. Starch is an organic material which is fully combustible and leaves the body porous after firing. Bovine bone ash is composed of porous grains which remains embedded in fired clay matrix and adds to the overall porosity of membranes.

Experimental Procedure

Raw Materials

Membranes were produced with clay labelled MY3 (collected from Mayouom-West Cameroon), plastic clay KG (from Koutaba-West Cameroon), cassava starch (AM) and bovine bone ash (OB). Each clay (MY3 and KG) had homogeneous texture during sampling. They have not yet been exploited by any industry and are located on deposits occupying a larger surface area and an average depth of 10 m (for MY3) and 3 m (for KG). Heavy particles, such as stone and quartz, were removed from MY3 by wet sieving at 125 μm. According to Njoya *et al.*[32] quartz constitutes ~6% of the total mass of MY3 clay. MY3 and KG were then dried at room temperature until constant weight and then at 100°C for 48 h. KG was crushed and sieved through a 125 μm sieve. Cassava starch was directly extracted from cassava collected from the plantation (at Matachom, West-Cameroon). After extraction, it was dried at 100°C in open air for 48 h, crushed with a corn mill (local device used to crush maize and cassava), and sieved at 125 μm. Bovine bones were collected from butcher shops. The samples were cut in small pieces, cleaned, and dried at 100°C in open air for 48 h. The dried bones were burned at 700°C for 2 h to reduce their hardness, then crushed and sieved with a 125 μm sieve. In each membrane paste, MY3 was the main material, KG was used as plasticizer and binder, AM and OB were used as pore-forming agents.

Particle size distributions of raw materials were analysed by laser granulometry using Mastersizer 2000 (Malvern Panalytical SARL, Almelo, Netherlands). Each measurement was carried out at dry state for a period of 5 s, at a pressure of 3 bars and a vibration rate of 30%. For each material, a cycle of two measurements was carried out with 2 s interval between the measurements.

Chemical compositions of MY3, KG, AM and OB were obtained by X-ray fluorescence spectroscopy (XRF). XRF was performed on pearls using a ZETIUM PANalytical spectrometer (Malvern Panalytical SARL, Almelo, Netherlands). A pearl is a glass disc obtained after fusion of a mixture of material and flux at 1060°C. The melting occurred in a LeNeo Claisse Fluxer brand furnace (Claisse, Quebec, Canada) and the flux used was lithium borate.

Phase analyses of MY3, KG and OB were obtained by X-ray diffractometry (XRD), performed on 100°C dried samples for an acquisition time of 52 min using a Bruker AXS D8 Advance diffractometer having a theta/theta goniometer (Bragg-Brentano geometry) with a copper anode producing CuKα (λ=1.5406 Å) radiation (40 kV, 40 mA) and a linear detector VANTEC-1. All samples analyzed by XRD were in powder form.

To detect the functional groups present in AM and OB, Fourier transform infrared spectroscopic (FTIR) analyses (between 400 and 4000 cm^{-1}) were carried out by KBr method using a Vertex 70 spectrometer (Bruker, Germany) on the pressed pellets, prepared by mixing 0.099 g of KBr with 0.001 g of sample powder.

Thermogravimetric and differential scanning calorimetric (TG/DSC) curves of the air-dried samples were recorded using a TG/DSC NETZSCH STA 449 F3 Jupiter (NETZSCH, Selb, Germany); ~20 mg of sample was placed in a platinum crucible in the microbalance and was heated from 30° to 1200°C (for AM and OB) and till 1400°C (for MY3 and KG). Analyses were performed under 20 $mL.min^{-1}$ supplied argon flow and at a heating rate of $5°C.min^{-1}$.

Description of Membrane Production

The process of membrane preparation included mixing, pressing, drying and sintering (Fig. 1). Four batches (CM0, CM1, CM2, CM3) were prepared by dry mixing of raw materials in different proportions as depicted in Table I,

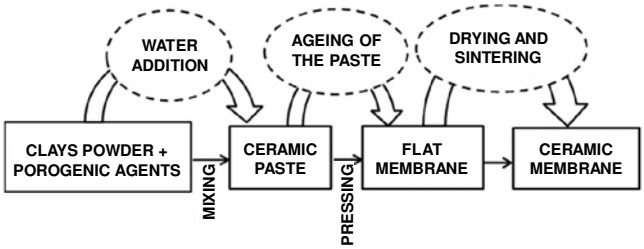

Fig. 1 – Membranes elaboration process

Table I : Different batch compositions for membrane preparation

	MY3 (%)	KG (%)	Pore-forming agents		Distilled water (%)
			AM (%)	OB (%)	
CM0	90	10	0	0	20
CM1	70	10	20	0	20
CM2	70	10	10	10	20
CM3	70	10	0	20	20

and ~20% (w/w) of distilled water were added to each batch to favor particles agglomeration. Mixing was done manually and the mixtures were kept at room temperature in a closed box for 24 h under high humidity to avoid premature drying and to ensure complete diffusion of water. Different ceramic membranes were shaped by uni-directional pressing of the mixtures through Specac hydraulic press (Eurolabo, Paris, France). CM0 did not contain any pore-forming agent and was considered as reference support. Prepared membranes were dried at room temperature till constant mass, then in an oven at 105ºC for 24 h. After drying, the membranes were sintered for 2 h at 1000º, 1050º, 1100º and 1150ºC in a Nabertherm brand oven (Nabertherm GmbH, Lilienthal, Germany). The heating rates were 2ºC/min from room temperature to 700ºC and 5ºC/min from 700ºC to the desired sintering temperature. The supports were designated as per the function of formulation and sintering temperature (Table II). Characterizations were done only on sintered membranes; green membranes were not characterized.

Table II : Designation of ceramic membranes

Primary samples	Designation of ceramic membranes after sintering at			
	1000ºC	1050ºC	1100ºC	1150ºC
CM0	CM01	CM02	CM03	CM04
CM1	CM11	CM12	CM13	CM14
CM2	CM21	CM22	CM23	CM24
CM3	CM31	CM32	CM33	CM34

Characterization of Membranes

Mineral compositions of different membranes were determined by XRD analysis. The analyses were performed on membranes sintered at 1000º and 1150ºC. These two temperatures were chosen in order to observe a significant change of the mineral phase. The analyses were carried out under the same conditions as for MY3, KG and OB.

Flexural resistance tests of different membranes produced at different temperatures were performed by using three points bending method using Instron 3369 instrument and Instron Bluehill Lite software (Instron, Norwood MA, USA). For each support, the scope and crosshead speed were 40 mm and 0.1 mm.min^{-1}, respectively.

Corrosion test was done using aqueous solutions of sulfuric acid (0.02 M, pH=1.68) and sodium hydroxide (0.17 M, pH = 13.24) at ~100ºC, and the reactions were carried out for 3, 6, 9 and 12 h. At the end, samples removed from the acid and base solutions were put in distilled water for a few minutes, then cleaned with ultrasound for 10 min, and dried at 105ºC for 72 h. The degree of corrosion was determined by the percentage of weight loss. Corrosion test was carried out to evaluate the aptitude of produced membranes to resist against strong acidic and basic attack. This method was used by Rekik *et al.*[15] Despite the fact that they are now used in neutral medium, the same membrane can be used to treat industrial wastewater which can be acidic or basic.

Scanning electron microscopic (SEM) analyses of 1000º and 1150ºC fired membranes were performed to determine the particles cohesion and surface quality. The apparatus used was JEOL JSM-IT300 (JEOL Ltd, Akishima, Tokyo, Japan). The surface of the ceramic membranes were coated with platinum for 30 s and observed in high vaccum mode.

Porosity, water absorption, and density were measured by using the Archimedes method. Pore size distribution and average pore size were determined from SEM images by using the 'Ruler' function of the apparatus and on polished sections of the membrane samples. The average pore size D (μm) was calculated using Eqn (1):

$$D = \sqrt{\frac{\sum_{i=1}^{n} n_i \times d_i^2}{\sum_{i=1}^{n} n_i}} \qquad ..(1)$$

where n is the number of pores and d_i is the diameter (μm) of each pore.

Frontal microfiltration tests were performed on a laboratory scale filtration pilot (Fig. 2). The porous membranes (CM04 and CM34) with diameter of 6.85 cm, filtration area of 36.83 cm^2 and thickness of 0.65 cm were placed on the membrane house filter (each at a time) and water was filled in the system from top. The experiment was carried out at room temperature (25º±3ºC) and atmospheric pressure. The membranes were conditioned by immersion in distilled water for a minimum of 24 h before the filtration test.

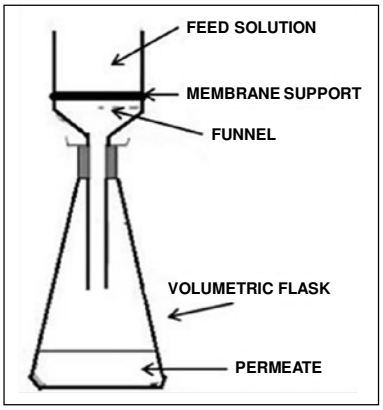

Fig. 2 – Frontal filtration pilot

Water permeability was measured by using distilled water and membranes produced at 1050º, 1100º and 1150ºC. The aim was to determine the water flux. Membranes obtained at 1000ºC were not used because CM11 did not have mechanical resistance and had many defects (such as crack). Distilled water was used to

observe the membranes' behavior when the liquid phase did not contain any particle. Crossing time (appropriate time for the passage of the first drop) and cumulative filtrated volume of water (every 10 min for 1 h) were measured.

Performance of membranes was examined by purification of polluted water prepared in the laboratory. The feed solution was prepared directly with local clay (KG) sieved at 125 μm and without any dispersing agent. 3 g of KG was mixed with 1 L of tap water. The mixture was stirred in a beaker with a magnetic stirrer for 5 h and settled for 24 h to obtain a feed solution with contaminant particles diameter <2 μm according to Stokes' law. The effluent solution was characterized by measuring physical parameters such as pH, conductivity, dissolved salt, dissolved oxygen, oxydo-reduction potential and turbidity. The apparatus used to measure these factors were Turbidity Meter PCE-TUM 20 for turbidity and PCE-PHD 1 for other analyses. The percentage of reduction (R_i) of each parameter was used to determine the performance of membranes.

$$R_i = \frac{i_{effluent} - i_{nfiltrate}}{i_{effluent}} \times 100 \qquad ..(2)$$

where $i_{effluent}$ and $i_{nfiltrate}$ represent each measured parameter in effluent and in filtrate water, respectively.

Results and Discussion

Powders Characterization

Particle size distribution of raw materials (Fig. 3) showed that MY3, KG and AM were constituted by small particles with respective d_{90} values of 33.55, 47.07 and 30.80 μm, while OB had the highest sized particles (d_{90}=111.59 μm).

Chemical compositions of MY3, KG, AM and OB (Table III) revealed that silica and alumina were the major components for MY3 and KG, while bovine bone ash (OB) was constituted mainly of calcium oxide and phosphorus pentoxide. The value of loss on ignition was 99.92% for starch (AM), and so, it could be completely consumed during the sintering of membranes. As an organic material, its combustion produced CO_2 which contributed to pore creation.

The FTIR spectrum of bovine bone ash annealed at 700°C for 2 h is presented in Fig. 4a. It was revealed earlier that the FTIR spectra of bone annealed between 700° and 1000°C exhibited the characteristic absorption peaks of hydroxyapatite (HAp).[33] In general, the FTIR spectrum of

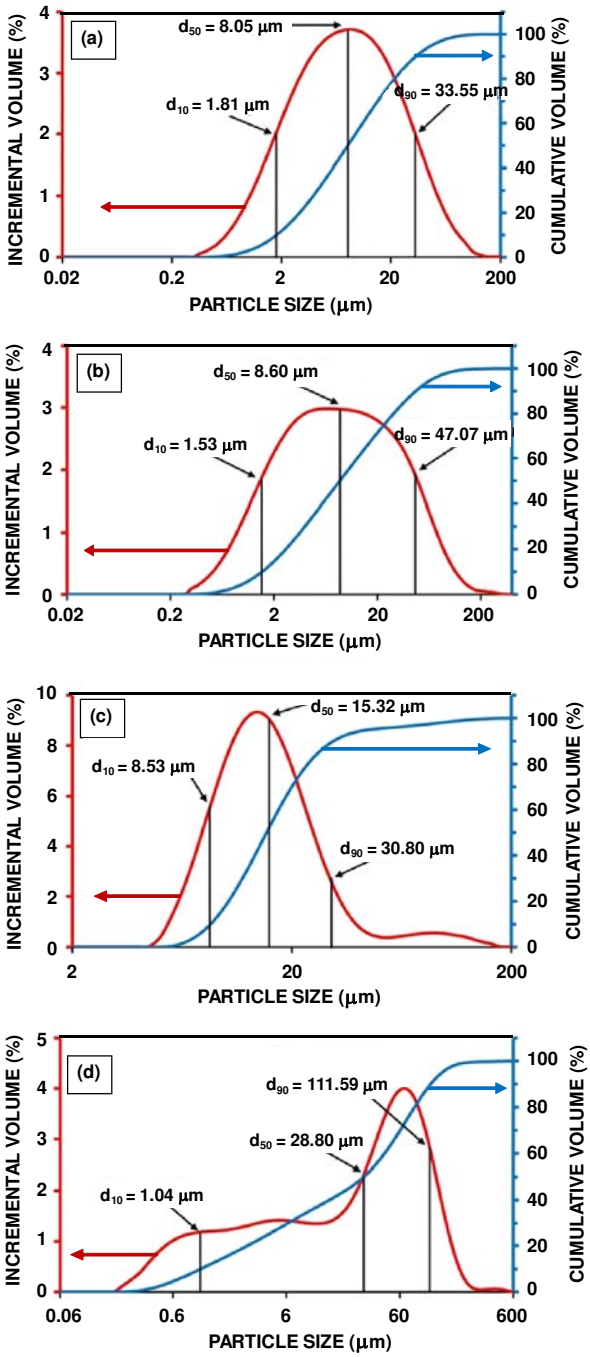

Fig. 3 – Particle size distribution of raw materials: (a) MY3, (b) KG, (c) AM, and (d) OB

Table III : Chemical compositions of the raw materials

Raw materials	Constituents (wt%)									
	SiO_2	Al_2O_3	Fe_2O_3	TiO_2	MgO	K_2O	Na_2O	CaO	P_2O_5	LOI
MY3	48.52	32.24	1.51	2.36	0.28	1.16	–	0.05	0.19	13.69
KG	59.48	22.26	3.44	1.56	0.38	0.33	–	0.15	0.07	12.33
OB	0.20	0.14	0.07	–	1.01	0.07	1.05	51.96	39.20	6.30
AM	0.02	0.01	0.01	–	–	0.01	–	0.01	0.01	99.92

annealed bovine bone ash showed the presence of carbonate (CO_3^{2-}), phosphate (PO_4^{3-}) and hydroxyl (OH^-) ions. The bands at 2014, 1459, 1417 and 875 cm^{-1} can be attributed to CO_3^{2-} ions,[33] bands at 1022, 962, 605, 567 and 472 cm^{-1} can be ascribed to PO_4^{3-} ions,[33] and the band at 3575 cm^{-1} corresponded to stretching vibration of hydroxyl ion (OH^-) of HAp.[33–35, 36] The bands observed at 3475 and 1638 cm^{-1} were due to the stretching vibration of crystal water and bending vibration of surface absorbed water, respectively.[37] Bands observed at 3575, 2014, 1459, 1417, 1022, 962, 875, 605, 567 and 472 cm^{-1} confirmed the HAp formation after sintering of bovine bone at 700ºC for 2 h. The FTIR spectrum of cassava starch (Fig. 4b) and bands assignment showed that it was constituted mainly of C, H and O. The bands at 3442, 2936 and 1660 cm^{-1} can be attributed to stretching vibration of O-H, and those at 1466 and 1460 cm^{-1} can be ascribed to bending vibrations of C-H.[38, 39] The results were in good agreement with those of XRF analysis. The loss on ignition (99.92%) can therefore be justified by the hydrocarbon character of AM.

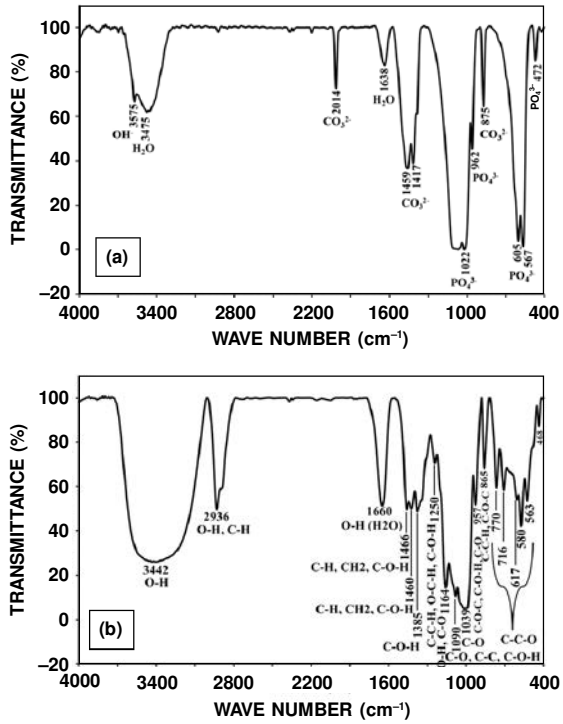

Fig. 4 – FTIR spectra of (a) bovine bone annealed at 700°C and (b) cassava starch

XRD patterns of MY3 and KG (Figs. 5a and 5b) showed the presence of kaolinite, quartz and anatase in the clay samples; kaolinite being more abundant in MY3 than in KG. In addition, MY3 showed the presence of illite and goethite, while KG showed the presence of montmorillonite and rutile. XRD pattern of KG (Fig. 5b) did not show any peak of iron mineral despite the high quantity of Fe_2O_3 given by XRF. The low peak intensity of montmorillonite might be due to dehydration of the sample during the drying step. XRD result of OB (Fig. 5c) showed that it was

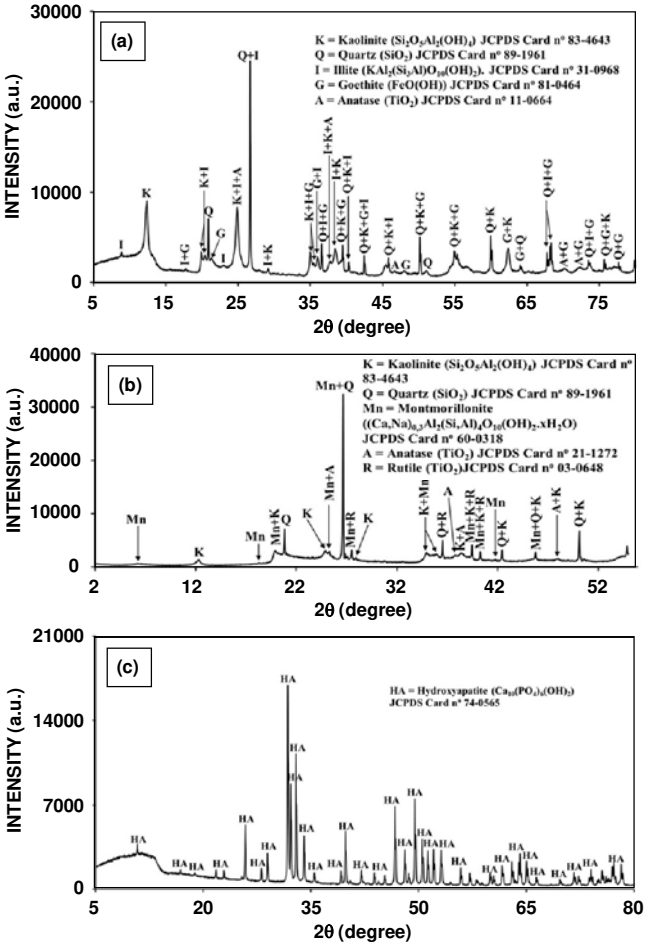

Fig. 5 – XRD patterns of (a) MY3, (b) KG, and (c) OB

basically constituted of HAp, confirming the result obtained by XRF analysis that bovine bone ash (OB) was mainly constituted of CaO and P_2O_5.

Thermal analyses of raw materials (Fig. 6) showed many endo and exothermic mass losses. TG curve of MY3 (Fig. 6a) showed a weak mass loss at 30º 200ºC due to moisture loss and a major mass loss at 340º 790ºC due to endothermic dehydroxylation to produce metakaolin. DSC curve of MY3 (Fig. 6a) indicated polymorphic transformation of α-quartz to β-quartz at 566ºC; the exothermic peak observed at 950º 1020ºC can be ascribed to the formation of crystalline phase. TG/DSC curves of KG (Fig. 6b) showed same phenomena as those of MY3 at almost similar temperatures, except the exothermic mass loss at 250º 380ºC due to organic combustion and dehydroxylation of goethite. TG/DSC curves of AM (Fig. 6c) showed an endothermic mass loss at 30º-110ºC due to moisture loss, and three endothermic peaks between 190º and 320ºC due to organics combustion; more than 74% of dry AM mass were lost at 240º-600ºC. TG/DSC curves of OB (Fig. 6d) showed a low mass loss due to the first thermal treatment of the material; the weak endothermic mass loss observed before 400ºC was due to moisture loss and early HAp dehydration which continued up to 900ºC.

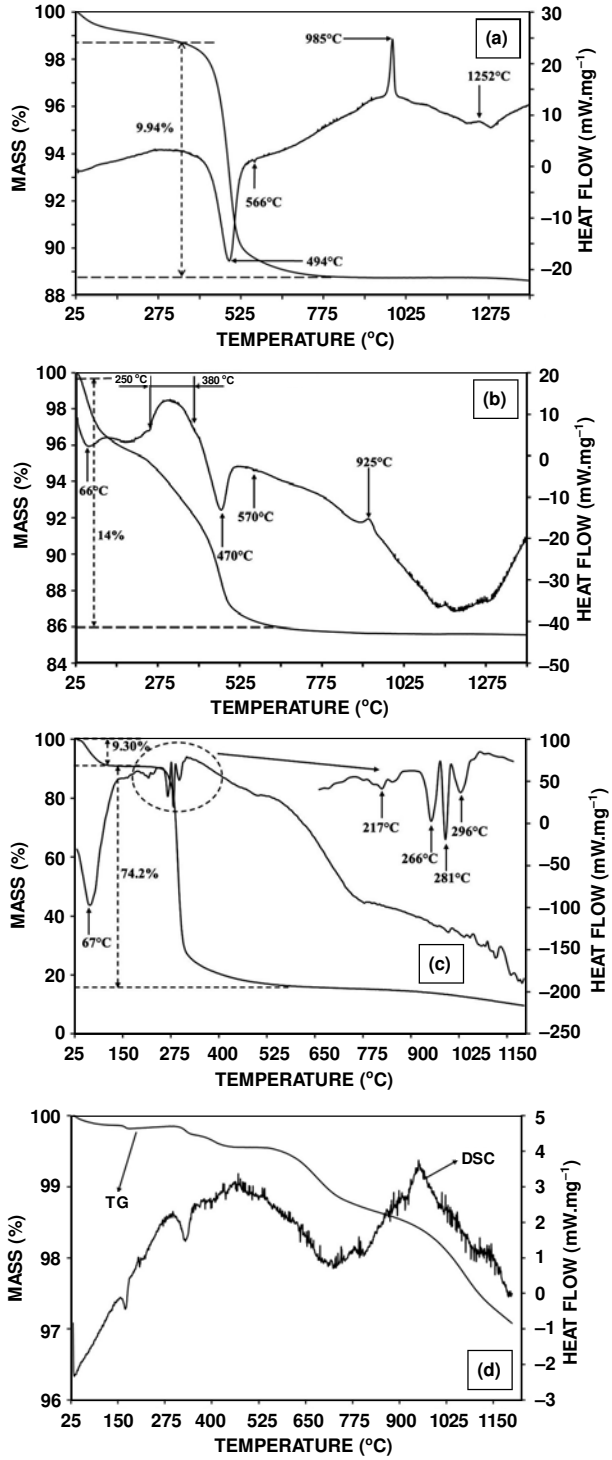

Fig. 6 – TG/DSC data for (a) MY3, (b) KG, (c) AM, and (d) OB

Membrane Characterization

The efficiency of the prepared microfiltration ceramic membranes were examined by studying their several properties such as porosity, water absorption, membrane morphology, mechanical resistance, chemical stability and permeability. The fabricated membranes (Fig. 7) had an average diameter of 72 mm and a thickness of 6 mm before sintering.

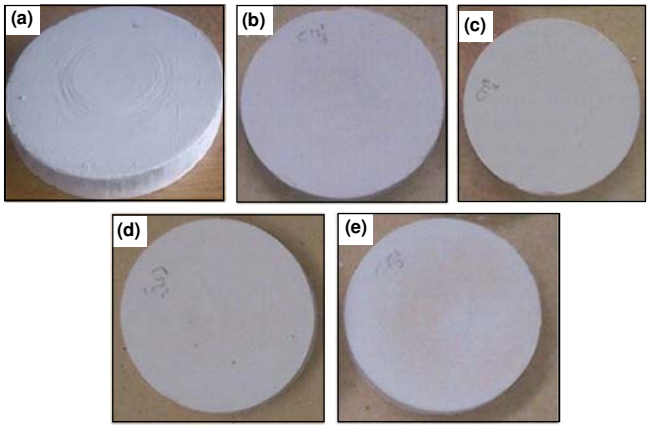

Fig. 7 – Flat microfiltration ceramic membranes' views: (a) after drying at 105°C; after baking at (b) 1000°C, (c) 1050°C, (d) 1100°C and (e) 1150°C

Mineralogy and Microstructure

XRD patterns of the membranes (Fig. 8) showed that the new phases formed were anatase, wustite and mullite. The formation of mullite (from kaolinite) was observed at 1150°C for all the samples. The quartz remained unchanged and it was the major mineral component after sintering at 1000°C. Anatase incorporated into the crystal structure of quartz or kaolinite appeared after the sintering. Wustite appeared from the thermal treatment of goethite. For supports which contained bovine bone ash, there were progressive formations of HAp. At higher temperature, HAp embedded in clay matrix became more compact through sintering and thus contributed to the solidification of membrane structures, increase of their flexural strength and reduction of porosity (Table IV).

The morphologies of different membranes, sintered at 1000° and 1150°C, can be studied from their SEM images (Fig. 9). As observed from the SEM images, there is no defect on the support surfaces. CM0 was less dense and had porous structure at 1000°C. This porosity decreased at 1150°C with appearance of inter-granular contacts. CM1, which contained only starch as pore-forming agent, showed highly porous structures at both the sintering temperatures. The membrane morphology showed granule formation, however, inter-granular contacts were very weak. Low particles aggregation of CM3 was observed at 1000°C, whereas at 1150°C this specimen became denser. This evolution of microstructure can be due to the presence of HAp delivered by bovine bone ash (Fig. 8). Despite the high particle aggregation of CM3, the open structure of the sample was still observed. For CM2, SEM revealed granule formation and weak inter-granular contacts at 1000°C. There were many pores of various sizes. At 1150°C inter-granular contacts became more pronounced and consequently aggregated to form large sizes without hindering the pore formation. Microstructures of different membranes revealed that 1150°C was the ideal sintering temperature and the specimens containing only bovine bone ash as pore-forming agent were denser than those

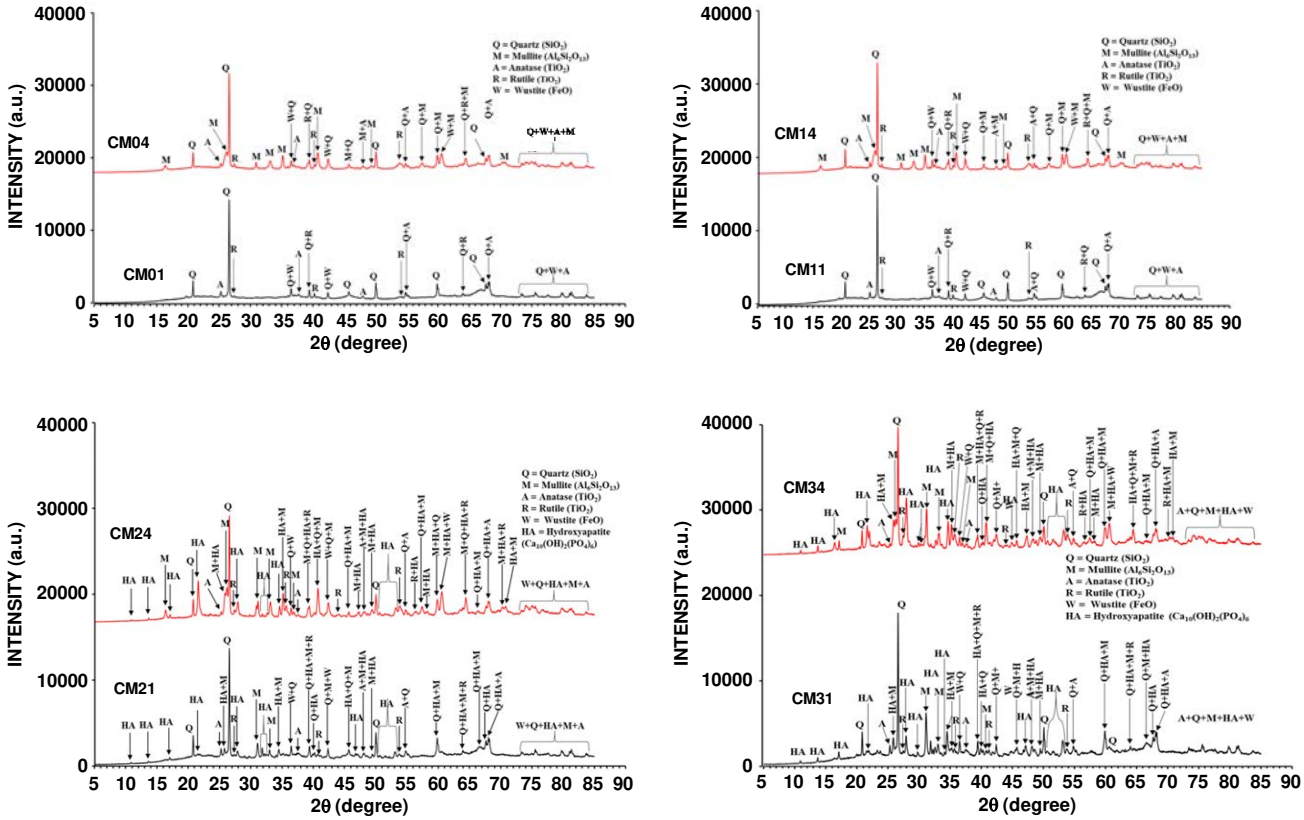

Fig. 8 – XRD patterns of elaborated ceramic membranes

Table IV : Physical characteristics of ceramic membranes

Samples	Porosity (%)	Water absorption (%)	Flexural strength (MPa)
CM01	39.06	24.02	1.98
CM02	39.57	24.34	2.12
CM03	34.57	19.74	5.02
CM04	31.83	17.41	7.45
CM11	54.42	44.93	1.07
CM12	55.45	46.74	1.10
CM13	48.78	44.19	1.26
CM14	52.03	39.91	1.54
CM21	48.89	35.10	3.77
CM22	48.55	34.54	2.39
CM23	44.02	29.20	2.73
CM24	40.03	24.55	3.17
CM31	36.91	21.25	6.06
CM32	34.53	19.20	3.62
CM33	46.25	31.41	1.70
CM34	36.09	20.74	7.79

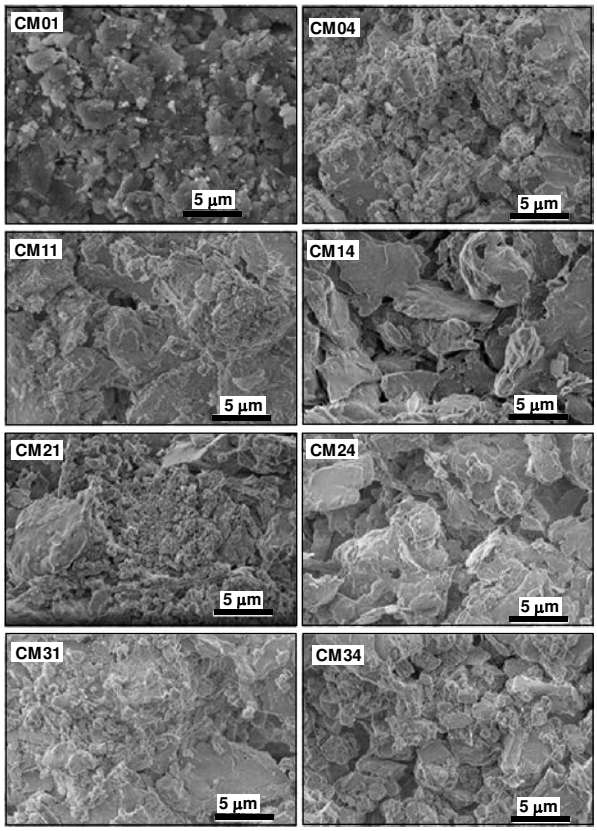

Fig. 9 – SEM images of ceramic membranes sintered at 1000°C and 1150°C

containing only starch or the mixture of two porogenic agents. Thus, cassava starch was a better porogenic agent than bovine bone ash.

Major visible pores in the SEM images were measured by using the 'Ruler' function of the apparatus. This function is used to measure the size of each pore present on the surface of the membranes.[24] The average pore size *D* (μm) was calculated using Eqn (1). Over 100 open pores were examined to determine the distribution and the average pore size of each membrane. The average pore sizes of the membranes resulted between 0.153 and 0.226 μm (Fig. 10), which revealed that the ceramic membranes were macroporous and hence could be used for microfiltration. Membrane, which contained only cassava starch as pore-forming agent (CM1), had higher average pore sizes (0.226 μm at 1000°C and 0.221 μm at 1150°C). Reference support CM0 had average pore sizes adjacent to that of support which contained the mixture of the porogenic agents (CM2). Membrane, which contained only bovine bone ash as pore-forming agent (CM3), had less average pore sizes (0.165 μm at 1000°C and 0.153 μm at 1150°C). Therefore, the addition of OB reduced the pore size. This can be due to the formation of HAp (Fig. 8), which also acted as binder at a higher temperature.

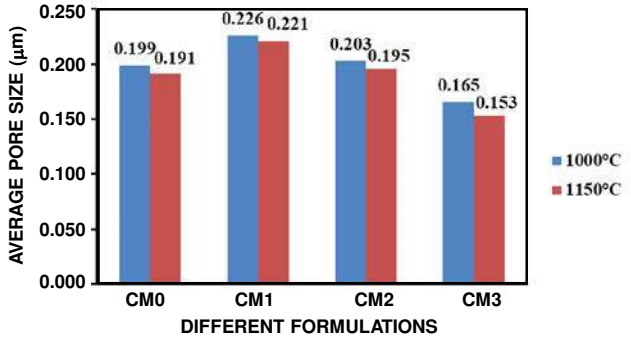

Fig. 10 – Average pore sizes of ceramic membranes sintered at 1000°C and 1150°C

Physico-Chemical and Mechanical Properties

Firing shrinkage (LS) gave values less than 7% (Fig. 11). The mass loss (ML) due to sintering was lower than 30% (Fig. 11). CM14, which was rich in starch, had higher firing shrinkage and mass loss; these confirmed that during sintering organic matter from starch and those contained in clay minerals were released. The slight mass loss observed for CM3 might be due to the fact that the bovine bone lost a considerable mass during thermal pre-treatment at 700°C.

The evolution of porosity as a function of sintering temperature (Table IV) showed that CM11 and CM12 had highest porosity (54% and 55%, respectively) and water absorption (45% and 46%, respectively), and CM04 had the lowest porosity (31%) and water absorption (17%). The high porosity of CM0 membrane may be due to the fact that particles were not well assembled up to 1150°C. Incorporation of bovine bone ash reduced the porosity at

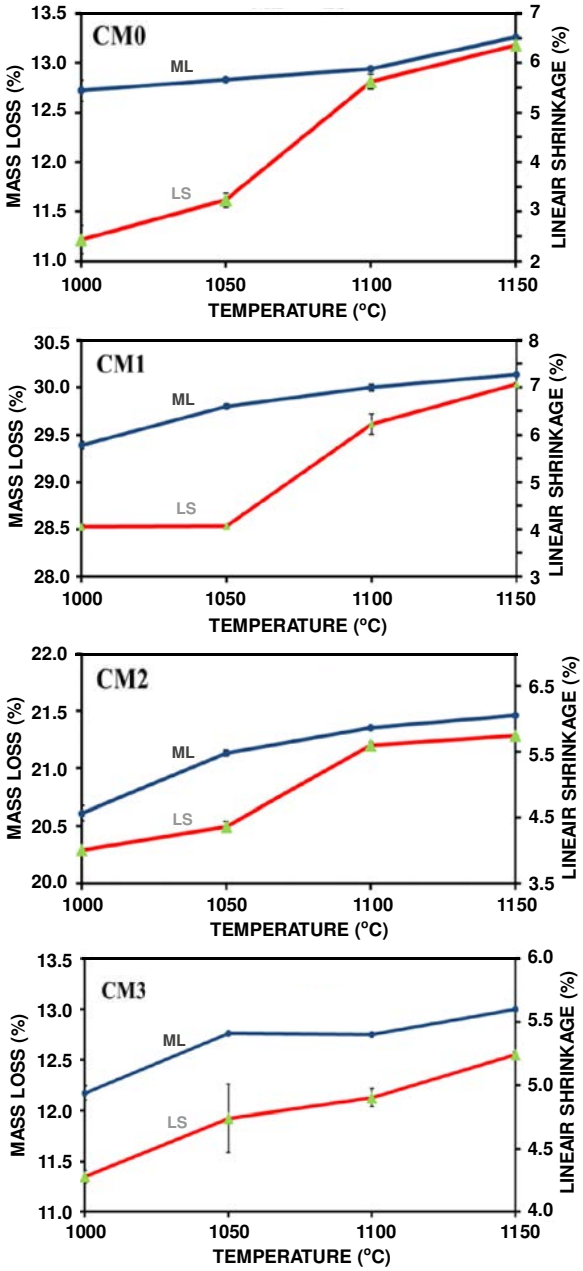

Fig. 11 – Variation of firing shrinkage (LS) and weight loss (ML) with sintering temperature

1000° and 1050°C, while increased the porosity at 1100° and 1150°C. Porosity is sensitive to firing temperature. The high values of porosity and water absorption of CM11, CM12 and CM14 might be due to massive departure of starch (as observed from the results of mass loss during sintering) in the form of CO_2. Other researchers also obtained similar porosity values in their study. For example, Arzani *et al.*[12] obtained 50.9% porosity, Rekik *et al.*[15] obtained porosity between 35% and 49%, Saffaj *et al.*[19] obtained porosity between 37% and 50% and Talidi *et al.*[18] obtained porosity between 31% and 47%. Comparing the result obtained in this study with those obtained by other researchers it can be inferred that membranes obtained at 1150°C were suitable for water and wastewater treatment.

Generally, mechanical resistance grows with temperature. Samples containing cassava starch as porogenic agent had low flexural strength values at all the temperatures (Table IV) due to their high porosities. For specimens, which contained mixture of the porogenic agents, the flexural strength was highest at 1000ºC (3.77 MPa), because firing at this temperature gave the specimen more compact morphology than those fired at higher temperatures (Fig. 9). For samples with bovine bone ash as porogenic agent, sintering at 1150ºC gave the highest flexural strength value (7.79 MPa) (Table IV); at this temperature the appearance of HAp (Fig. 8) lead to a denser microstructure (Fig. 9).

According to the results obtained through corrosion test (Fig. 12), the weight loss was proportional to the time of reaction and inversely proportional to the sintering temperature. The weight loss also varied with the reaction medium (acidic or basic). The highest corrosion rate (5.96%) was obtained after a basic attack of CM11 for 12 h; the main mineral of CM11 was quartz (SiO_2), which was acid, and hence, reacted easily in basic medium. The lowest corrosion rate (0.04%) was observed with an acidic attack of CM04 for 3 h. Analysis of the results showed that despite the nature of the membrane, a sample with high porosity had a high corrosion rate and that with low porosity had low corrosion rate. As cassava starch rendered more pores, the corrosion rates were high for CM1 specimens (Fig. 12), hence corrosion of such membranes was favoured in both the media. Rekik *et al.*[15] and Majouli *et al.*[40] obtained chemical resistance of <6% after acidic and basic attacks at different temperatures and medium concentration. Considering the results obtained by those authors, it can be stated that membranes developed in the present work had a high resistance to chemical corrosion and can be used in acidic and basic media.

Ultimately, the sintering temperature and nature of porogenic agents has an important effect on membrane properties. Thermal treatment done at 1150ºC gave better results for the overall microfiltration membranes. At this sintering temperature, chemical resistance was high (low degree of corrosion), mechanical resistance was acceptable, porosities were in the range of those obtained by many authors. Ceramic membranes produced with bovine bone ash were dense and had fewer pores, small pore size, good chemical and mechanical resistance. Despite their good chemical resistance, small pore size and acceptable porosity, starch (AM) membranes, due to their less dense microstructure, presented low flexural strength resistance, which can be improved by reducing the proportion of cassava starch in the membrane

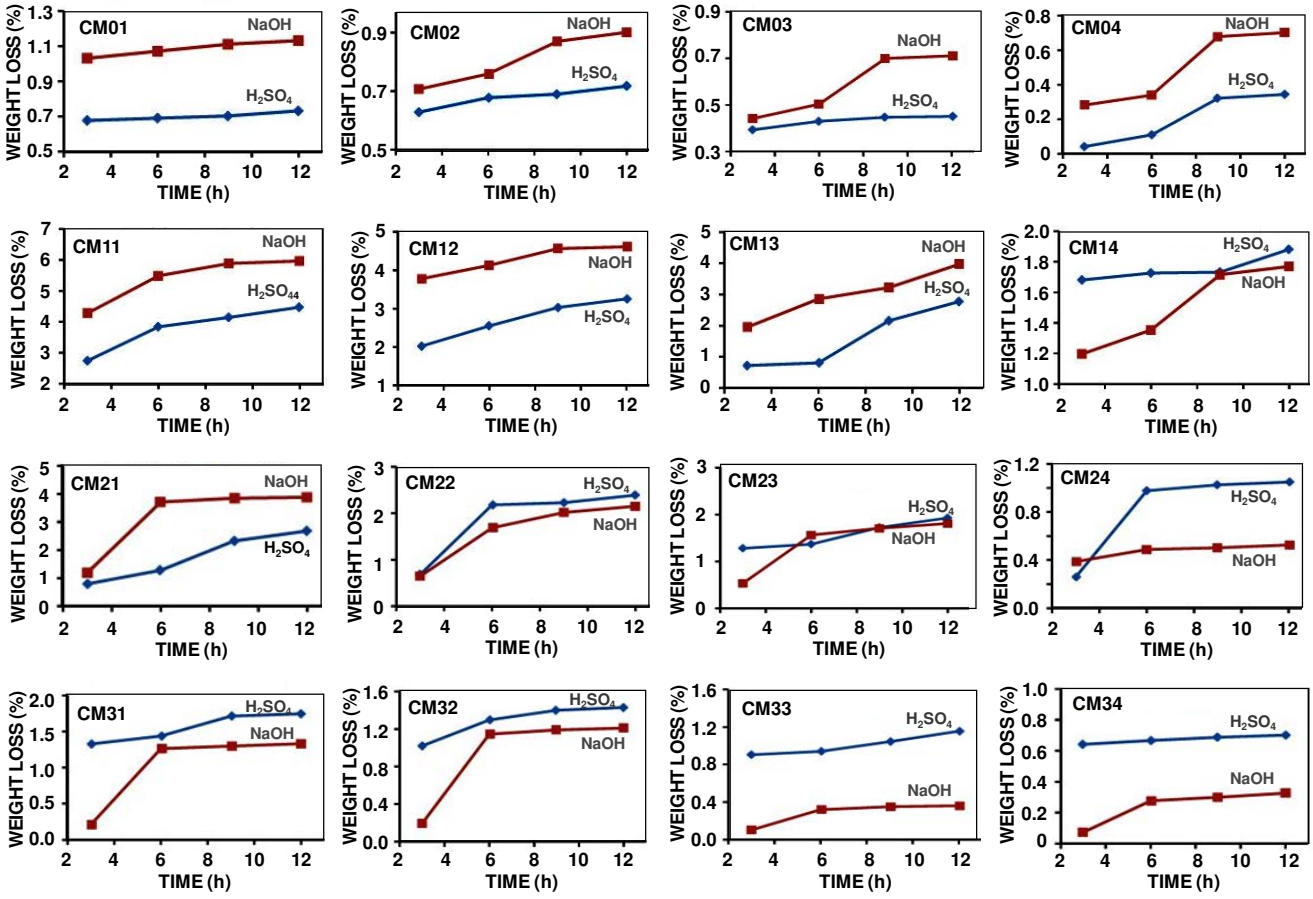

Fig. 12 – Weight loss of ceramic membranes in sulphuric acid (pH = 1.68) and soda solution (pH = 13.24) as a function of time at 105ºC

formulation. Membranes with mixture of porogenic agents rendered better microstructure, physicochemical and mechanical properties than the AM membranes. Thus, membranes which can be used for good water filtration are those obtained without a porogenic agent, with bovine bone ash, with the mixture of the two pore-forming agents, and fired at 1150°C. These membranes are CM04, CM24 and CM34.

Microfiltration Test

To determine the water permeability of the membranes produced at 1050°, 1100° and 1150°C, cumulative filtrated volumes of distilled water were plotted against filtration time, which gave quasi-linear curves for all the membranes (Fig. 13). The increase of filtrated volume with time was predictable because the fluids did not contain any particle to fill the available pores and thereby reduce the filtration rate or stop it progressively. The crossing time (time required for the first drop to cross the support) varied from one support to another. The highest crossing time was obtained with CM03 (100 min) and the lowest was obtained with CM14 (1 min), which contained the highest surface pore size (Fig. 10).

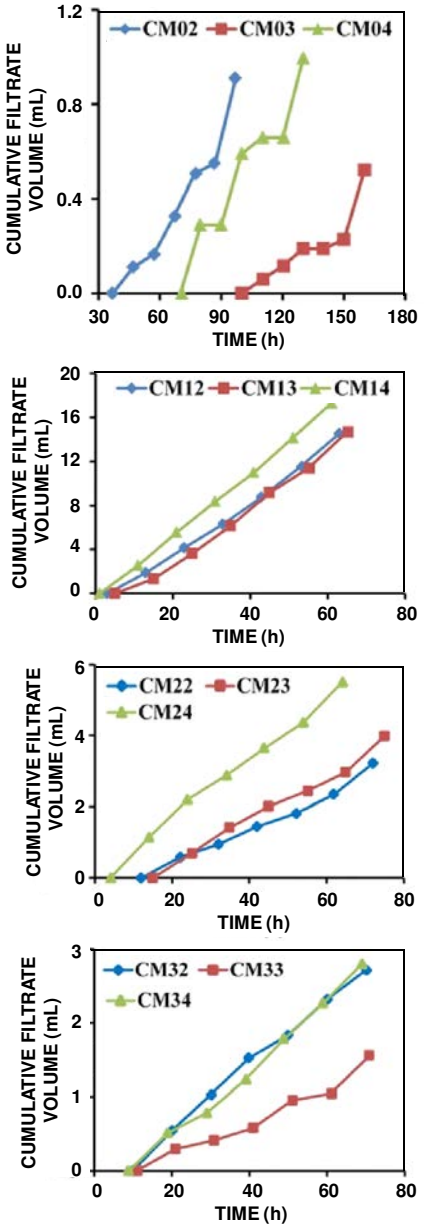

Fig. 13 – Distilled water cumulative filtrate volume versus filtration time

The frontal filtration tests of contaminated water gave interesting results. The characteristics of water before and after filtration (Table V) showed that performances of the two membranes (CM04 and CM34) were different. The pH reduced from low basic value (8.21) to neutral value (7.36 for CM04 and 7.51 for CM34). The higher value of pH obtained with CM34 can be explained by the presence of HAp and CaO, which was a basic oxide. CM04, which was rich in acid and amphoteric oxide (SiO_2 and FeO), reduced the pH more than CM34. This result confirmed that supports influenced the pH of filtered water. Filtration results also showed that CM04 support could reduce up to 97.70% of turbidity, 81.08% of conductivity, 85.71% of dissolved salts, 36.00% of dissolved oxygen, whereas CM34 could reduce up to 99.26% of turbidity, 90.62% of conductivity, 85.71% of dissolved salts and 44.00% of dissolved oxygen. So, for all the physical parameters, CM34 exhibited higher rejection factor than CM04 (Table V), despite its higher porosity than CM04 (Table IV). This may be attributed to the lower mean pore size of CM34 (0.153 μm) than CM04 (0.191 μm) (Fig. 10). During the water clarification test, the pore size played a selective role and the membrane with the smallest pores had the highest rejection factor. The turbidity rejection factors obtained in this work (97.70% for CM04, 99.26% for CM34) were close to those obtained by many authors. For example, Achiou *et al.*[24] removed 99.40% turbidity by filtering effluent from textile industry, Barrouk *et al.*[14] achieved 96.00% and 99.00% rejection of residual dye by using microfiltration and ultrafiltration membrane, respectively, and Mouiya *et al.*[41] removed up to 99.80% turbidity by filtering several effluents from different origins. However, the rejection rate of oily wastewater filtration obtained by Eom *et al.*[1] (84.10%, 84.20% and 86.10%) were less than those obtained in this work.

Table V : Characteristics of effluent and filtrated water

Properties		pH	Conductivity (mS/cm)	Turbidity (NTU)	Dissolved salt (%)	Dissolved oxygen (mg/L)
Effluent		8.21	1.396	77	0.07	2.50
CM04	$i_{permeate}$	7.36	0.264	1.77	0.01	1.60
	R_i (%)		81.08	97.70	85.71	36.00
CM34	$i_{permeate}$	7.51	0.131	0.57	0.01	1.40
	R_i (%)		90.62	99.26	85.71	44.00

The appearance of effluent and filtrated water showed that water colouration changed after filtration from brown to colourless (Fig. 14). This change confirmed that filtration through CM04 and CM34 membranes improved the quality of the studied effluent. The evaluation of frequency of use and study of recycling techniques of theses membranes will permit to appreciate their real performance. These studies will be carried out during the next works in addition to this one.

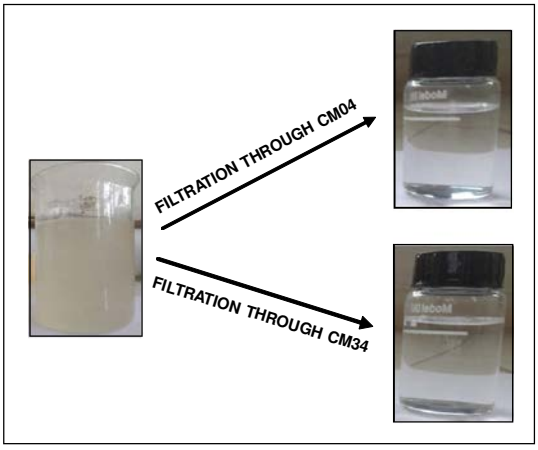

Fig. 14 – Effluent water and permeate

Conclusions

The objective of this work was to prepare microfiltration ceramic membranes with good physicochemical and morphological properties using low-cost clay minerals and to compare the effects of temperature as well as of cassava starch and bovine bone ash on the studied properties. The prepared ceramic membranes were expected to have good mechanical and chemical resistances and high porosity (more than 30%). The low-cost membranes were developed by uniaxial pressing technique and sintering at 1000°, 1050°, 1100° and 1150°C for 2 h. Results showed that 1150°C was the ideal sintering temperature. CM04 had the lowest porosity (31.83%), CM24 had a well cumulative filtrates volume and CM34 had the highest flexural strength (7.79 MPa). According to the studied properties, like porosity, water permeability, filtration test, chemical resistance and mechanical resistance, the main objective of the present work was reached and the specimens with good performances which could be used as domestic ceramic membranes were CM04, CM24 and CM34. The results also proved that local clay, cassava starch and bovine bone ash were the appropriate materials for the elaboration of good microfiltration ceramic membrane.

Acknowledgements: The authors of this work express their sincere gratitude to the staff of Center of Analysis and Characterization of Marrakech (CAC) for their availability and support during this work. The financial support of Agence Universitaire de la Francophonie (AUF) is also gratefully acknowledged.

References

1. J.-H. Eom, H.-J. Yeom, Y.-W. Kim and I.-H. Song, *Clays Clay Miner.*, **63**, 222-234 (2015).
2. L. Basnayaka, N. Subasinghe and B. Albijanic, *Appl. Clay Sci.*, **156**, 45-52 (2018).
3. K. Prochaska, E. Konowal and J. Sulej-chojnacka, *Colloid. Surf. B: Biointerf.*, **74**, 238-243 (2009).
4. S. Li, C. Wang and J. Zhou, *Ceram. Adv. Energy Technol.*, **39**, 8833-8839 (2013).
5. W. Misrar, M. Loutou, L. Saadi, M. Mansori, M. Waqif and C. Favotto, *J. Asian Ceram. Soc.*, **5**, 199-208 (2017).
6. B. Shimekit, H. Mukhtar, F. Ahmad and S. Maitra, *Trans. Indian Ceram. Soc.*, **68**, 115-138 (2009).
7. S. Sarkar, *Trans. Indian Ceram. Soc.*, **73**, 239-244 (2014).
8. N. Saffaj, M. Persin, S. A. Younssi, A. Albizane, M. Bouhria, H. Loukili, H. Dacha and A. Larbot, *Sep. Purif. Technol.*, **47**, 36-42 (2005).
9. N. El Baraka, N. Saffaj, R. Mamouni, A. Laknifli, S. A. Younssi, A. Albizane and M. El Haddad, "Development and Characterization of Flat Membrane Supports Based on Moroccan Clay", pp. 1-8 in: *VII èmes Journées d'Etudes Techniques*, May 2-4, Marrakesh, Morocco (2012).
10. S. Sarkar, S. Bandyopadhyay, A. Larbot and S. Cerneaux, *J. Membr. Sci.*, **392-393**, 130-136 (2012).
11. S. K. Amin, H. A. M. Abdallah, M. H. Roushdy and S. A. El-Sherbiny, *Int. J. Appl. Eng. Res.*, **11**, 7708-7721 (2016).
12. M. Arzani, H. Reza, M. Sheikhi, T. Mohammadi and O. Bakhtiari, *Appl. Clay Sci.*, **161**, 456-463 (2018).
13. K. S. Ashaghi, M. Ebrahimi and P. Czermak, *Open Environ. J.*, **1**, 1-8 (2007).
14. I. Barrouk, S. A. Younssi, A. Kabbabi, M. Persin, A. Albizane and S. Tahiri, *J. Mater. Environ. Sci.*, **6**, 2190-2197 (2015).
15. S. B. Rekik, J. Bouaziz, A. Deratani and S. Baklouti, *J. Membr. Sci. Technol.*, **6**, 1-12 (2016).
16. M. B. Ali, N. Hamdi, M. A. Rodriguez, K. Mahmoudi and E. Srasra, *Ceram. Int.*, **44**, 2328-2335 (2018).
17. Y. Dong, B. Lin, J. Zhou, X. Zhang, Y. Ling, X. Liu, G. Meng and S. Hampshire, *Mater. Charact.*, **62**, 409-418 (2011).
18. A. Talidi, N. Saffaj, K. E. Kacemi, S. A. Younssi, A. Albizane and A. Chakir, *Sci. Stud. Res.: Chem. Eng. Biotechnol. Food Ind.*, **12**, 263-268 (2011).
19. N. Saffaj, M. Persin, S. Alami, A. Albizane, M. Cretin and A. Larbot, *Appl. Clay Sci.*, **31**, 110-119 (2006).
20. P. B. Belibi, S. Cerneaux, M. Rivallin, M. B. Ngassoum and M. Cretin, *J. Appl. Chem.*, **3**, 1991-2003 (2014).
21. O. Qabaqous, N. Tijani, M. N. Bennani and A. El Krouk, *Mater. Environ. Sci.*, **5**, 2244-2249 (2014).
22. H. Alghamdi, A. Dakhane, A. Alum and M. Abbaszadegan, *Mater. Des.*, **152**, 10-21 (2018).
23. B. Ghouil, A. Harabi, F. Bouzerara, B. Boudaira, A. Guechi, M. M. Demir and A. Figoli, *Mater. Charact.*, **103**, 18-27 (2015).
24. B. Achiou, H. Elomari, M. Ouammou, A. Albizane, J. Bennazha, S. A. Younssi, I. E. El Amrani and A. Aaddane, *J. Mater. Environ. Sci.*, **7**, 196-204 (2016).

25. N. Saffaj, N. El Baraka, R. Mamouni, H. Zgou, A. Laknifli, S. A. Younssi, Y. Darmane, M. Aboulkacem and O. Mokhtari, *J. Microbiol. Biotechnol. Res. Sch*., **3**, 1-6 (2013).

26. M. L. Sandoval, M. H. Talou, A. G. Tomba, M. A. Camerucci, E. Gregorová and W. Pabst, *Ceram. Int*., **44**, 3893-3903 (2018).

27. A. Norhayati, B. M. Maisarah, A. A. Muhd, Z. Nurhanna and I. F. Ahmad, *J. Teknol. Sci. Eng*., **69**, 117-120 (2014).

28. N. Saffaj, H. Loukili, S. A. Younssi, A. Albizane, M. Bouhria, M. Persin and A. Larbot, *Desalination*, **168**, 301-306 (2004).

29. E. Kamseu, C. Leonelli, D. N. Boccaccini, P. Veronesi, P. Miselli, G. Pellacani and U. C. Melo, *Ceram. Int*., **33**, 851-857 (2007).

30. D. Njoya, M. Hajjaji, A. Baçaoui and D. Njopwouo, *Mater. Charact*., **61**, 289-295 (2010).

31. O. R. Njindam, D. Njoya, J. R. Mache, M. Mouafon, A. Messan and D. Njopwouo, *Constr. Build. Mater*., **170**, 512-519 (2018).

32. A. Njoya, C. Nkoumbou, C. Grosbois, D. Njopwouo and D. Njoya, *Appl. Clay Sci*., **32**, 125-140 (2006).

33. C. Y. Ooi, M. Hamdi and S. Ramesh, *Ceram. Int*., **33**, 1171-1177 (2007).

34. N. A. M. Barakat, M. S. Khila, A. M. Omran, F. A. Sheikh and H. Y. Kim, *J. Mater. Process. Technol*., **209**, 3408-3415 (2009).

35. W. Khoo, F. M. Nor, H. Ardhyananta and D. Kurniawan, *Proc. Manuf*., **2**, 196-201 (2015).

36. A. Szcze, Y. Yan, E. Chibowski, L. Holysz and M. Banach, *Appl. Surf. Sci*., **434**, 1232-1238 (2018).

37. F. Mohandes, M. Salavati-niasari, M. Fathi and Z. Fereshteh, *Mater. Sci. Eng. C*, **45**, 29-36 (2014).

38. B. H. Holder, Dissertation & Thesis in Food Science and Technology, p. 94, University of Nebraska-Lincoln, Lincoln, NE, USA (2012).

39. B. C. Huang, R. Jeng, M. Sain, B. A. Saville and M. Hubbes, *Biores*., **1**, 257-269 (2006).

40. A. Majouli, S. A. Younssi, S. Tahiri, A. Albizane, H. Loukili and M. Belhaj, *Desalination*, **277**, 61-66 (2011).

41. M. Mouiya, A. Abourriche, A. Bouazizi, A. Benhammou, Y. El Hafiane, Y. Abouliatim, L. Nibou, M. Oumam, M. Ouammou, A. Smith and H. Hannache, *Desalination*, **427**, 42-50 (2018).